Magneto-optics of two-dimensional electron gases modified by strong Coulomb interactions in ZnSe quantum wells

D. Keller,[1] D. R. Yakovlev,[2,3] G. V. Astakhov,[1,3] W. Ossau,[1] S. A. Crooker,[4] T. Slobodskyy,[1] A. Waag,[5] G. Schmidt,[1] and L. W. Molenkamp[1]

[1]*Physikalisches Institut der Universität Würzburg, 97074 Würzburg, Germany*

[2]*Experimentelle Physik 2, Universität Dortmund, 44221 Dortmund, Germany*

[3]*A. F. Ioffe Physico-Technical Institute, Russian Academy of Sciences, 194021 St. Petersburg, Russia*

[4]*National High Magnetic Field Laboratory, Los Alamos, New Mexico 87545, USA*

[5]*Institute of Semiconductor Technology, Braunschweig Technical University, 38106 Braunschweig, Germany*

(Received 20 September 2005; revised manuscript received 11 October 2005; published 5 December 2005)

The optical properties of two-dimensional electron gases in ZnSe/(Zn,Be)Se and ZnSe/(Zn,Be,Mg)Se modulation-doped quantum wells with electron densities up to 1.4×10^{12} cm^{-2} were studied by photoluminescence, photoluminescence excitation, and reflectivity in a temperature range between 1.6 and 70 K and in external magnetic fields up to 48 T. In these structures, the Fermi energy of the two-dimensional electron gas falls in the range between the trion binding energy and the exciton binding energy. Optical spectra in this regime are shown to be strongly influenced by the Coulomb interaction between electrons and photoexcited holes. In high magnetic fields, when the filling factor of the two-dimensional electron gas becomes smaller than 2, a change from Landau-level-like spectra to exciton-like spectra occurs. We attempt to provide a phenomenological description of the evolution of optical spectra for quantum wells with strong Coulomb interactions.

DOI: 10.1103/PhysRevB.72.235306 PACS number(s): 78.66.Hf, 71.10.Ca, 71.35.−y, 78.67.De

I. INTRODUCTION

Optical spectroscopy is a powerful tool in studying the energy spectrum of electronic states in low-dimensional heterostructures. It was successfully used for investigation of two-dimensional electron gases (2DEG) (for review see e.g., Ref. 1), providing additional information not available from transport measurements alone. However, in optical experiments the presence of photoexcited holes perturbs the energy spectrum of the 2DEG via electron-hole Coulomb interactions, an effect which should be taken into account for proper interpretation of optical spectra. This is already the case for III-V semiconductor heterostructures based on GaAs, where the Coulomb interaction is relatively weak (e.g., the exciton binding energy in bulk GaAs is 4.2 meV). However, Coulomb interactions are of major importance for II-VI semiconductors (e.g., the exciton binding energy in bulk ZnSe is 20 meV). Modification of the optical spectra of modulation-doped quantum wells (QW) containing a 2DEG has been the subject of extensive theoretical[2–10] and experimental studies.[11–27]

In undoped QWs, the ground state of an optically excited single electron-hole pair is an exciton (X), which is formed by the Coulomb interaction between the electron and the hole. For QWs with a very dilute two-dimensional electron gas where the electron concentration $n_e \ll 1/\pi a_B^2$ (here a_B is the radius of the quasi-two-dimensional exciton), a negatively charged exciton complex is the energetically lowest excitation.[28–31] The negatively charged exciton is composed of two electrons and a hole, and is commonly called a trion (T), and is analogous to the negatively charged H^- state of the hydrogen atom. In semiconductor QWs trions have binding energies of a few meV and are observed in optical spectra below the exciton resonance. In the limit of zero-electron concentration, the energy separation between trion and exciton optical transitions corresponds to the binding energy of "isolated" trions E_B^T (i.e., the trion state which is not perturbed by the interaction with the 2DEG). It varies usually from 5–20 % of the exciton binding energy E_B^X depending on the QW thickness and the height of the barriers (see, e.g., Ref. 32, and references therein).

For a high density 2DEG with $n_e \geqslant 1/\pi a_B^2$, screening and phase space filling effects destroy the strong Coulomb attraction between an individual electron and hole, i.e., the exciton formation is suppressed.[2] As a result, instead of a narrow excitonic emission, a broad emission band with a linewidth determined by the 2DEG Fermi energy ε_F is characteristic of this regime. Also, a Fermi-edge singularity (FES) appears in optical spectra owing to the Coulomb interaction of a photocreated hole with the electrons at the Fermi surface.[5,11] Optical spectra are usually interpreted in terms of band-to-band transitions, dressed with many-body interactions of the excited or annihilated electron-hole pair with electrons of the Fermi sea.[2] The energies of the emission and absorption thresholds are shifted following a band-gap renormalization. Extended numerical calculations are needed to model optical spectra of a QW with a dense 2DEG. On the basis of such calculations Hawrylak *et al.* predicted the presence of two thresholds (two peaks) in the absorption spectrum corresponding to the bound states of the photoexcited hole interacting with a 2DEG. The first threshold occurs at an energy $\hbar\omega_1$ and is a doubly occupied trion complex. The second threshold with an energy $\hbar\omega_2$ corresponds to an exciton created in the 2DEG.[6,7,33] This approach allows one to explain the main features in the optical spectra of modulation-doped GaAs QWs.[7,8]

Evolution of the optical spectra with increasing electron density from the low-density to the high-density limit is an

important issue which has been examined experimentally in recent years for GaAs (Ref. 34), CdTe (Refs. 16, 17, 22, and 23) and ZnSe (Refs. 21 and 24) based QWs. General trends have been established and attempts to formulate a phenomenological description have been undertaken. It has been shown that for all studied material systems the filling factor $\nu=2$ separates Landau-level-like behavior from an excitonic-like behavior in external magnetic fields. In high magnetic fields for $\nu<2$ the broad emission band transforms into a narrow line that shifts diamagnetically, reminiscent of the trion line in low-doped samples. Further field increase to $\nu<1$ revives one more line in optical spectra, which is excitonic-like. In these fields, optical spectra of moderately doped and very weakly doped QWs look identical. Despite the considerable progress in experiment the situation is still far from being completely understood, in major part due to the absence of a proper model description of the intermediate concentration regime. In this regime with $0.05/\pi a_B{}^2 \leq n_e \leq 1/\pi a_B{}^2$ the Fermi energy of the 2DEG falls in the range between the trion and exciton binding energies $E_B^T \leq \varepsilon_F \leq E_B^X$, and the effect of the Coulomb interaction on the optical spectra can be discussed in terms of comparing these three characteristic energies.

ZnSe-based QWs exhibit very strong Coulomb electron-hole interactions (the exciton binding energy is twice as large as compared to CdTe QWs and four times larger than in GaAs QWs). The Coulomb energy amounts to 30–40 meV. In earlier studies of *n*-type doped (Zn,Cd)Se/ZnSe QWs the well layers were made of ternary alloy (Zn,Cd)Se.[25–27] This results in a considerable broadening of optical lines by alloy fluctuations which obscures fine details in the spectroscopic analysis.

In this paper we present a comprehensive optical study of *n*-type modulation-doped ZnSe/(Zn,Be,Mg)Se QWs, with an aim to investigate the modification of optical spectra in structures with strong Coulomb interactions, and at the intermediate electron densities satisfying the condition $E_B^T \leq \varepsilon_F \leq E_B^X$. Photoluminescence (PL), PL excitation (PLE), and reflectivity spectra have been measured in high magnetic fields up to 48 T. We found that in low and moderate magnetic fields the optical spectra behave along a phenomenological description suggested by the traditional band-to-band model. However, there are some data, like the absolute energies of optical transitions, the emergence of excitonlike resonances in high magnetic fields, and the presence of combined electron-exciton processes at small filling factors, which the traditional model cannot explain at all. At present there is no universal approach that explains the intermediate range of electron densities and we attempt here to develop a phenomenological picture of experimental appearances to be accounted for by a theoretical description.

The paper is organized as follows. In Sec. II details of the sample structure and the experimental techniques are described. In Sec. III optical spectra at a zero magnetic field are discussed. The modification of optical spectra in high magnetic fields is presented in Sec. IV. In Sec. V we summarize the experimental results by giving a phenomenological picture.

TABLE I. Parameters of the samples containing a ZnSe QW with $Zn_{0.82}Be_{0.08}Mg_{0.10}Se$ and $Zn_{0.94}Be_{0.06}Se$ barriers. For QW widths the nominal values are given.

Sample	QW width (Å)	Barrier material	Barrier gap E_g^b (eV)	Electron density (cm^{-2})	Fermi energy ε_F (meV)
#1*R*	67	(Zn,Be,Mg)Se	3.06	3×10^{10}	0.5
#1*D*	67	(Zn,Be,Mg)Se	3.06	5×10^{11}	7.7
#2*R*	100	(Zn,Be)Se	2.93	8×10^{10}	1.2
#2*D*	100	(Zn,Be)Se	2.93	1.4×10^{12}	21.5

II. EXPERIMENTAL DETAILS

ZnSe/(Zn,Be,Mg)Se quantum wells were grown at the University of Würzburg by molecular-beam epitaxy on (100)-oriented GaAs substrates. Detailed growth parameters for these structures can be found in Ref. 35. We list some of them here for convenience and some parameters are collected in Table I. The band gap of ZnSe at a liquid helium temperature is 2.82 eV, the band gaps of the barrier materials E_g^b are given in the Table. The band gap discontinuity between the QW and barrier is distributed between the conduction and valence band in the proportion $\Delta E_C/\Delta E_V=78/22$. The electron effective mass in ZnSe is $m_e=0.15m_0$ and the heavy-hole in-plane mass is $m_h=0.46m_0$. The exciton binding energy is $E_B^X \approx 30$ meV and the trion binding energy is $E_B^T \approx 5$ meV.

Two sets of samples have been studied, each consisting of a modulation-doped quantum well (QW) labeled with "*D*" and a nominally undoped reference QW labeled with "*R*" (see Table I and schema in Figs. 1 and 2). The samples in each set were grown under identical conditions, except for the modulation doping with iodine donors in the barrier layer, which provides a 2DEG in the QW.

Samples 1*R* and 1*D* from the first set have a 67-Å-thick ZnSe single quantum well embedded between 1000-Å-thick $Zn_{0.82}Be_{0.08}Mg_{0.10}Se$ barriers. To prevent the loss of carriers escaping into the substrate and recombining at the surface, this structure was clad between 500-Å-thick $Zn_{0.71}Be_{0.11}Mg_{0.18}Se$ barriers with wider band gap. Sample 1*D* has two 20-Å-thick iodine-doped layers, symmetrically placed in the $Zn_{0.82}Be_{0.08}Mg_{0.10}Se$ barriers and separated from the QW by 100-Å-thick spacers. The electron density in this QW of 5×10^{11} cm^{-2} was evaluated by the nonmonotonic behavior of the optical spectra in the vicinity of integer filling factors[20,21,36] (the results will be collected in Fig. 8). This electron density corresponds to a Fermi energy of $\varepsilon_F=7.7$ meV. In ZnSe QWs ε_F (meV)$=n_e\pi\hbar^2/m_e=2.3\times10^{-12}n_e$ (cm^{-2})$/(m_e/m_0)$. The electron density 3×10^{10} cm^{-2} in the reference sample 1*R* is due to unintentional doping of the thick barrier layers, which provides free electrons for the single QW. The density was evaluated from the ratio of the trion and exciton oscillator strengths.[37] Note, due to possible technological inaccuracy the well width in sets 1*R* and 1*D* could be slightly different from nominal. We evaluate them from the quantum-confinement shift of the *X* optical transition (Ref. 35) as 61 Å in 1*R* and 67 Å in 1*D*.

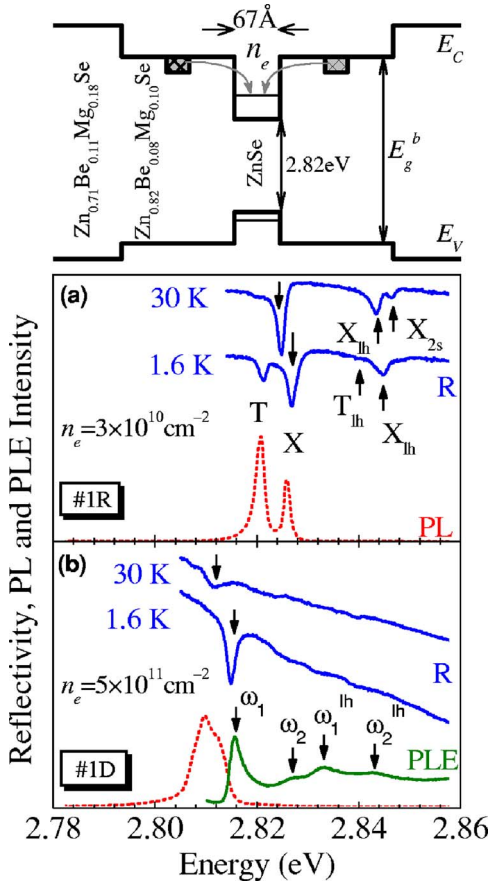

FIG. 1. (Color online) Photoluminescence (PL), photoluminescence excitation (PLE), and reflectivity (R) spectra of two 67-Å-thick ZnSe/$Zn_{0.82}Be_{0.08}Mg_{0.10}Se$ QWs, with different electron densities: (a) reference QW 1*R* with $n_e=3\times10^{10}$ cm^{-2}, (b) doped QW 1*D* with $n_e=5\times10^{11}$ cm^{-2}. $B=0$ T, and $T=1.6$ K. Scheme shows a sketch of samples type 1.

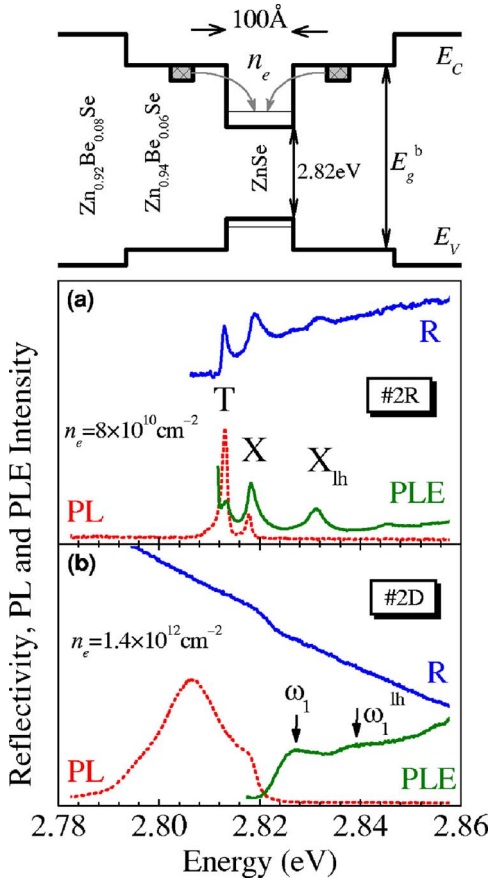

FIG. 2. (Color online) Photoluminescence (PL), photoluminescence excitation (PLE), and reflectivity (R) spectra of two 100-Å-thick ZnSe/$Zn_{0.94}Be_{0.06}Se$ QWs, with different electron densities: (a) reference QW 2*R* with $n_e=8\times10^{10}$ cm^{-2}, (b) doped QW 2*D* with $n_e=1.4\times10^{12}$ cm^{-2}. $B=0$ T, and $T=1.6$ K. Scheme shows a sketch of samples type 2.

This problem has not been recognized for set 2.

Samples 2*R* and 2*D* have a 100-Å-thick ZnSe single QW embedded between 1000-Å-thick $Zn_{0.94}Be_{0.06}Se$ barriers that are further sandwiched between additional 500-Å-thick $Zn_{0.92}Be_{0.08}Se$ barriers. The residual electron density in 2*R* is 8×10^{10} cm^{-2}. Similar to 1*D* the modulation-doped layers in 2*D* consist of 20-Å-thick layers symmetrically located on both sides of the well at a distance of 100 Å. This sample has a higher electron density 1.4×10^{12} cm^{-2} and, respectively, a larger Fermi energy of $\varepsilon_F=21.5$ meV. We note here that both doped samples satisfy the condition $E_B^T \leqslant \varepsilon_F \leqslant E_B^X$.

Photoluminescence, PLE, and reflectivity spectra were measured in external magnetic fields applied perpendicular to the QW plane (Faraday geometry). Circularly polarized components of these spectra were analyzed in order to resolve states with different spin configurations and spin orientations. Experiments in magnetic fields up to 8 T were performed in Würzburg in a split-coil superconducting solenoid and for temperatures from 1.6 to 70 K. A midpulse magnet (~400-ms decay) at the National High Magnetic Field Laboratory (Los Alamos, USA) was used for experiments up to 48 T performed at a temperature $T=1.6$K. Details of the pulsed magnet setup are given in Ref. 38. Photoluminescence was excited by UV lines of an Ar-ion laser (Würzburg) or by a He-Cd laser with a photon energy of 3.8 eV (Los Alamos). For the photoluminescence excitation measurements a dye laser (stilbene-3) was used. Excitation density was kept below 10 W/cm^2, to exclude considerable heating of the 2DEG. In reflectivity experiments a halogen lamp was used as a light source. Spectra were measured by a liquid-nitrogen-cooled charge-coupled-device detector associated with either a 1-m or 0.3-m spectrometer.

III. OPTICAL SPECTRA AT A ZERO MAGNETIC FIELD

First we discuss properties of PL, PLE, and reflectivity spectra in the absence of external magnetic fields, which are given in Fig. 1 for the samples 1*R* and 1*D*.

A PL spectrum from the undoped 1*R* sample measured at $T=1.6$ K is shown in Fig. 1(a) by a dashed line. It consists of two narrow lines, each with a full width at half maximum (FWHM) of 1.4 meV. The linewidth is due to inhomogeneous broadening, caused by fluctuations of the QW width and alloy fluctuations of the barrier material. The line at 2.8259 eV labeled as *X* is related to the 1s state of the heavy-hole exciton. The trion line (*T*) is shifted by 5.1 meV to

lower energy from the neutral exciton X line. Identification of the charged and neutral exciton lines is based on magneto-optical spectra (for details see Refs. 31 and 35). Both exciton and trion transitions are also observable in reflectivity spectra [solid lines in Fig. 1(a)]. Due to its smaller binding energy the trion disappears rapidly with increasing temperature in emission and reflectivity spectra. However the exciton transition is broadened but remains observable up to room temperature. It is well established for QWs with low electron concentrations that the energy difference between the exciton and trion lines increases linearly with the Fermi energy.[16,35] The electron density of 3×10^{10} cm^{-2} in the 1R sample corresponds to ε_F=0.5 meV and, therefore, the binding energy of an "isolated" trion can be evaluated as E_B^T=5.1−0.5 =4.6 meV.

The light-hole exciton (X_{lh}) in the reflectivity spectrum of sample 1R is shifted by 18.7 meV to higher energies with respect to the heavy-hole exciton (X) due to strain and quantum confinement. The resonance of the light-hole trion (T_{lh}) at 2.8404 eV has a rather small oscillator strength. The binding energy of the light-hole trion of 3.7 meV is approximately 1 meV smaller than that of the heavy-hole trion which is in agreement with earlier reports.[31,35] A weak resonance at 2.8463 eV in the reflectivity spectrum at 30 K corresponds to the 2s-state of the heavy-hole exciton (X_{2s}). The energy difference between the 1s and 2s exciton of 21.6 meV is in a good agreement with the calculated value of 24.7 meV for the corresponding QW width.[35]

The PL spectrum of the corresponding doped sample (1D) is shown in Fig. 1(b). It consists of a broad band with a maximum at 2.810 eV and a shoulder at 2.812 eV. The FWHM of 7 meV is very close to the value of the 2DEG Fermi energy of 7.7 meV. The PL band has a sharp decrease of intensity at its high energy side. We will show below that the optical transitions at this spectral position of 2.814 eV involve electrons located in the vicinity of the Fermi level. These transitions correspond to the half-intensity point of the rising edge in PLE spectrum.

PLE and reflectivity spectra of sample 1D are dominated by strong narrow lines at 2.815 eV [labeled as ω_1 in Fig. 1(b)], which coincides with the high energy tail of the PL band. The width of the resonance in the reflectivity spectrum is about 2 meV and is equal approximately to the width of the exciton resonance in the 1R sample. It is a remarkable fact that at a low temperature of 1.6 K the reflectivity spectrum of the relatively highly doped structure is indistinguishable from the spectrum of the nominally undoped QW, where a single resonance of the neutral exciton dominates. Both the linewidth and the oscillator strength of the resonances in sample 1D are very similar to that of the exciton transition in undoped structures.[18] Temperature dependencies presented below disclose this similarity and reveal the difference in the origin of these resonances. At energies higher than the ω_1 line, three weak features can be distinguished in the PLE and reflectivity spectra. The first peak at 2.8273 eV(ω_2) is blueshifted by 11.8 meV with respect to the lowest absorption threshold ω_1. Note, this value is close to the $E_B^T+\varepsilon_F$ =12.3 meV. Transitions at 2.8332 and 2.8433 eV are ascribed to the corresponding light-hole resonances, ω_1^{lh} and ω_2^{lh}. The difference in their transition energies is 10.1 meV. This value equals again approximately the sum of the trion binding energy and the Fermi energy, which gives a value of 11.4 meV for the light-hole trion.

It should be noted here that the commonly accepted notation of the spectral features in the optical spectra of doped QWs is not settled yet. In this paper we will follow the approach using ω_1 and ω_2 resonances introduced by Cox *et al.* for the optical spectra of CdTe-based QWs in the regime $E_B^T \leqslant \varepsilon_F \leqslant E_B^X$.[16,22] This notification originates from the theoretical works of Hawrylak *et al.*, where it was however introduced for the regime of a high dense 2DEG with $\varepsilon_F > E_B^X$.[6,7] It is still an open question of how far this approach and the respective theoretical predictions can be extended to describe optical spectra in QWs with a 2DEG of lower density. As we will show here some of the qualitative predictions of the Hawrylak's theory are valid to describe our experimental observations. Namely, the theory predicts that the energy difference between two thresholds in absorption, ω_1 and ω_2, corresponding to bound states, satisfies the equality $\hbar\omega_2-\hbar\omega_1=E_B^T+\varepsilon_F$.[6] This relation holds for sample 1D.

Optical spectra from the second set of samples (2R and 2D) are shown in Fig. 2. In most regards, they are similar to the first set described above. The main difference comes from the higher electron density of sample 2D. The PL spectrum from the reference sample 2R consists of an exciton line (X) at 2.8178 eV and a trion line at 2.8131 meV with linewidths of 1.3 meV [see Fig. 2(a), dashed line]. Both transitions are observable as strong resonances in PLE and reflectivity spectra. Due to larger QW width and smaller barrier height compared to sample 1R, the energy splitting between the heavy-hole and light-hole excitons is only 13.3 meV.

The shape of the PL spectrum of the doped sample 2D is similar to that of 1D. The FWHM of the emission band in 2D is 17.8 meV, which is again in a good agreement with ε_F=21.5 meV. In contrast to 1D, the singularity at the fundamental absorption edge ω_1 of 2D is smeared out in the PLE spectrum and the half intensity point of the rising edge in the absorption (PLE) is blueshifted by 3.6 meV with respect to the high energy side of the PL band. Additionally, a weak absorption attributed to the ω_1^{lh} is observable in the PLE spectra 13 meV higher than the ω_1 line energy. In reflectivity spectra, the oscillator strength of both transitions is weak. We were not able to distinguish a second absorption threshold ω_2 for sample 2D. It is worth noting that even for such a high electron density $n_e=1.4\times10^{12}$ cm^{-2}, the energy position of the characteristic absorption and emission edges in sample 2D stay in the vicinity of the exciton and trion transitions of undoped and weakly doped samples of the same well width.

The shape of the PL spectrum of the doped samples is typical for modulation-doped QWs with high electron densities, where the optical transitions are interpreted as band-to-band transitions of free carriers (see Fig. 3). In this case, all electrons in a 2DEG can recombine with photoexcited holes. It is commonly suggested that the momentum conservation selection rule for optical transition (Δk=0) is partially relaxed due to scattering with the electrons of the 2DEG, or to collective excitations of the Fermi sea.[2] Photocreated holes

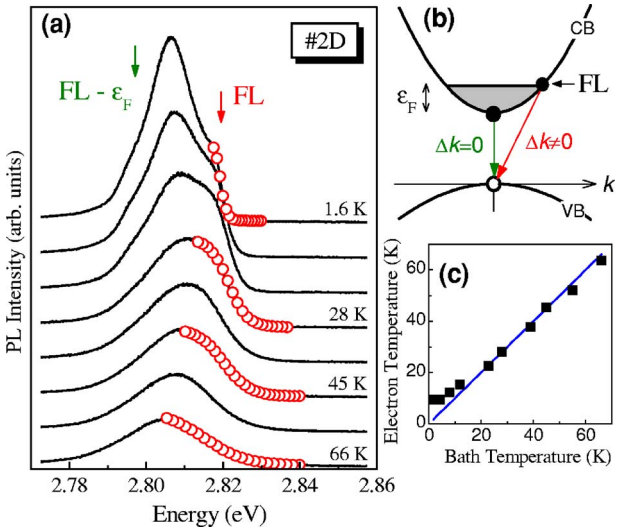

FIG. 3. (Color online) (a) PL spectra of the 2*D* sample with $n_e=1.4\times10^{12}$ cm^{-2} at different temperatures (solid lines). Circles represent a fitting of the high energy side of the spectra by a Fermi distribution using the electron temperature as a parameter. Arrows indicate indirect transition from Fermi level (FL) and from the bottom of conduction band (CB) FL$-\varepsilon_F$ to the top of valence band (VB). (b) A scheme of these transitions in the band-to-band model. Panel (c) shows the results of the fitting vs sample bath temperature.

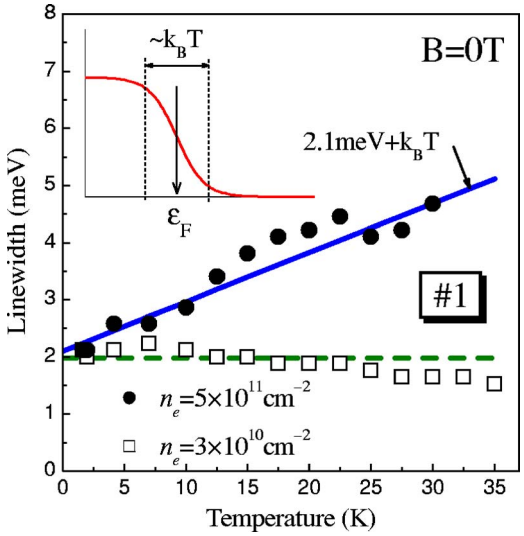

FIG. 4. (Color online) Temperature broadening of resonances in reflectivity spectra for undoped and doped ZnSe-based QWs. Squares represent data of the exciton broadening in sample 1*R*. Circles represent data for the ω_1 resonance in 1*D*. Lines are guide to the eye. The energy distribution of electrons in vicinity of the Fermi energy is shown schematically in the inset.

thermalize to the top of the valence band ($k=0$). As a result, indirect optical transitions with $\Delta k\neq0$ between the electrons of the conduction band and holes of the valence band contribute significantly to emission spectra [Fig. 3(b)]. We will show below that despite the visual similarity in the shape of emission spectra, this simple interpretation is insufficient to describe the optical spectra in the intermediate concentration regime where $E_B^T\leqslant\varepsilon_F\leqslant E_B^X$. Coulomb interactions and excitonic effects are of great importance in this regime.

The temperature dependence shown in Fig. 3(a) helps to clarify the origin of the PL band in the doped samples. It is seen that in sample 2*D* the line shape varies strongly as the bath temperature is increased from 1.6 up to 66 K. With the temperature increase, the maximum becomes less pronounced and also a shoulder on the high energy side smears out and becomes indistinguishable for temperatures higher than 30 K. Let us first concentrate on the shape of the high energy tail of the emission band. We have fit it with the Fermi function, and the results of the fit are indicated by circles. The electron temperature, used as a fitting parameter, is plotted as a function of the bath lattice temperature in Fig. 3(c). A solid line in the figure is a linear dependence with unity slope, i.e., it corresponds to the conditions when the electron temperature is equal to the bath temperature. One can see that most of the experimental points closely follow this dependence. This allows us to conclude that indeed the high energy tail of the emission band in doped 2DEGs is due to electrons in the vicinity of the Fermi level. The transition energy corresponding to the Fermi level derived from the fit procedure is shown in Fig. 3(a) by an arrow labeled FL at 2.819 eV for $T=1.6$ K. It corresponds to the energy where the luminescence intensity at the sharp high energy side has dropped down to 50% of its maximum value.

The linewidth of the emission band is also expected to be related to the properties of the 2DEG, namely to the Fermi energy ε_F. As can be seen from Fig. 3(b), depending on the hole distribution the emission linewidth should vary from $\varepsilon_F=21.5$ meV up to $(1+m_e/m_h)\varepsilon_F=28.5$ meV. The latter value was calculated with electron and hole masses $m_e=0.15m_0$ and $m_h=0.46m_0$, which have been inferred from the quadratic diamagnetic shift of the exciton line in sample 2*R* (see Ref. 35). Experimental data agreed well with this range. For low temperatures, where the line shape is complex, we label by an arrow in the figure the energy position of the expected low energy tail of the emission band at FL $-\varepsilon_F$. In the temperature range from 30 to 66 K the FWHM is 23.5 meV. The temperature evolution of the PL band in sample 1*D* is qualitatively similar to sample 2*D* and therefore the experimental data are not shown. Modeling of the line shape is a complicated task and is beyond the scope of this paper.

Temperature dependences are very helpful in highlighting the qualitative differences between the resonances in reflectivity spectra of doped and undoped samples. We note that at $T=1.6$ K, the broadening and the amplitude (i.e., resonance oscillator strength) of the resonances were very similar in these samples (see Fig. 1). However, a difference in the temperature broadening of the resonances in samples 1*R* and 1*D* is clearly seen in Fig. 4. The exciton resonance in the undoped sample 1*R* shows no temperature broadening for $T<35$ K. Significant temperature broadening of the exciton line is expected due to exciton scattering on LO phonons, which becomes important only for temperatures exceeding 100 K. In contrast, the width of the reflectivity resonance of the doped sample 1*D* increases linearly with temperature. The slope of this increase equals k_BT, which is expected for the Fermi statistics of the 2DEG in the vicinity of the Fermi

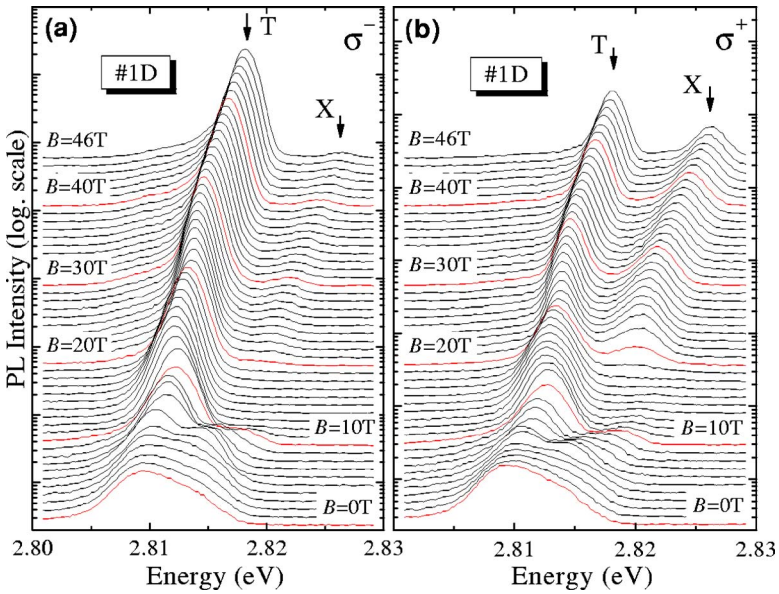

FIG. 5. (Color online) PL spectra from a doped 67-Å-thick $ZnSe/Zn_{0.82}Be_{0.08}Mg_{0.10}Se$ QW sample 1*D* with $n_e=5\times10^{11}$ cm^{-2} for magnetic fields varied from 0 to 46 T and $T=1.6$ K. (a) in σ^- polarization. (b) in σ^+ polarization.

level. This allows us to conclude that the strong resonance ω_1 in reflectivity and PLE spectra is due to the Coulomb interaction of the photoexcited holes and electrons in the vicinity of the Fermi edge. In other words it is due to an excitonic effect involving electrons at the Fermi level.

Let us summarize the results of optical spectra examined in the absence of external magnetic fields. Emission, reflectivity, and PLE spectra of the doped samples 1*D* and 2*D* are clearly controlled by the 2DEG and especially by the electrons in vicinity of the Fermi level. Their appearance agrees qualitatively with what is expected and commonly accepted for the highly-doped QWs with $\varepsilon_F > E_B^X$, a situation which is often described in terms of band-to-band optical transitions with negligible electron-hole Coulomb interactions. However, we study here II-VI heterostructures with strong Coulomb interactions and also examine an intermediate electron density regime characterized by $E_B^T \leqslant \varepsilon_F \leqslant E_B^X$. Is it clear from our experimental data that the high energy side of the emission spectra and the absorption edge, detected via reflectivity and PLE spectra, does not correspond to the energy of the optical transition from the valence band to the Fermi level. These characteristic energies are moved to lower energies by about 30 meV, which is the exciton binding energy, suggesting the importance of electron-hole Coulomb interactions. Schematically these characteristic energies are displayed in Fig. 12. We will discuss this schema and designation of the characteristic energies in more detail after presenting the results of magnetic field studies.

IV. MODIFICATION OF OPTICAL SPECTRA IN HIGH MAGNETIC FIELDS

A. PL spectra

We turn now to modifications of optical spectra in external magnetic fields. The evolution of the photoluminescence spectra from sample 1*D* is shown in Fig. 5 for σ^- (a) and σ^+ polarization (b). PL intensity is given in a logarithmic scale. The broad PL band that is characteristic at low magnetic fields [see also Fig. 1(b)] is transformed for $B>20$ T into two narrow lines which are very similar to the exciton and trion lines of the reference QWs. The polarization of the higher energy line, which resembles the exciton in the undoped structures, is opposite to the polarization of the trion. At low magnetic fields, the PL band splits into a set of lines, which shift almost linearly to higher energies with increasing field. Above 10.3 T, the linear energy shift of the lowest line converts into a quadratic diamagnetic shift typical for excitonic states. Details of this transformation are easier to follow on the fan-chart diagram given in Fig. 6(a). Similar behavior has been reported recently for GaAs-based QWs.[13,14] It was shown that the transformation occurs at a filling factor $\nu=2$ and that at high magnetic fields the emission is indistinguishable from trions. Theoretically, the transformation from a linear shift for $\nu>2$ to a quadratic diamagnetic shift for $\nu<2$ can be explained by a hidden symmetry, which can hold for $\nu<2$,[9] and the energy of optical transitions for $\nu<2$ resembles the energy of the exciton.

Figures 7 and 6(b) show the influence of the magnetic field on the luminescence spectra of the sample 2*D*. Field-induced changes of the spectra are similar to that of sample 1*D*. As a consequence of higher electron concentration, the characteristic transformation of the spectra appears at higher magnetic fields. For low magnetic fields, the high energy side of the luminescence band shows oscillations, due to the depopulation of higher Landau levels. These oscillations became very pronounced for filling factor $\nu=4$ at $B=14.5$ T. For filling factor $\nu=2$ at 29 T the trion-like luminescence is recovered. We do not reach here the regime of filling factor $\nu=1$, which is expected at $B=58$ T, i.e., beyond the maximum field available. As a consequence we do not observe the recovery of the exciton-like emission line, as was observed for sample 1*D* with lower electron density.

The 2DEG density in the modulation-doped samples was evaluated from oscillations of the optical properties at integer filling factors. With growing magnetic field the number of electrons in the uppermost occupied Landau level varies periodically. As a result many-body effects such as the elec-

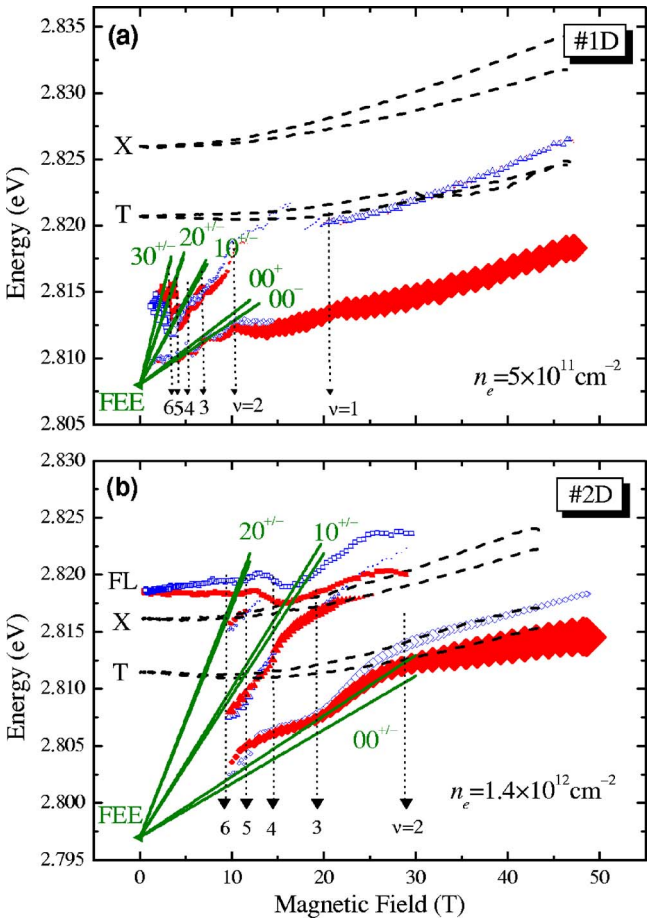

FIG. 6. (Color online) (a) Energy of PL maxima of a doped 67-Å-thick $ZnSe/Zn_{0.82}Be_{0.08}Mg_{0.10}Se$ QW $1D$ with $n_e=5\times10^{11}$ cm^{-2} vs magnetic field detected in σ^+ (open symbols) and σ^- (closed symbols) polarizations. Exciton (X) and trion (T) quadratic diamagnetic shifts for $1R$ sample are shown by lines. Landau level fan chart is shown for off-diagonal transitions with in-plane electron and hole effective masses of $m_e=0.15m_0$ and of $m_h=0.46m_0$, respectively. Vertical lines indicate magnetic fields of integer filling factors. The fundamental emission edge (FEE) at 2.808 eV corresponds to the low energy side of the luminescence band at $B=0$. (b) Same for a doped 100-Å-thick $ZnSe/Zn_{0.94}Be_{0.06}Se$ QW $2D$ with $n_e=1.4\times10^{12}$ cm^{-2} and the corresponding reference sample $2R$. Squares represent the energy of the transitions of electrons at the Fermi level (FL). The fundamental emission edge (FEE) is located at $E_{\mathrm{FEE}}=2.797$ eV. It is equal to the low energy side of the luminescence band FL$-\varepsilon_F$ at $B=0$ (see also Fig. 3). $T=1.6$ K.

tron exchange and correlation energy, the screening of the Coulomb interactions of the electron and hole, and the degree of spin polarization of the 2DEG oscillate with increasing magnetic field. The oscillations can be found in a variety of optical properties, such as the degree of circular polarization, the integrated intensity of luminescence, and the energy positions of the lines. These oscillations are especially pronounced in the vicinity of integer filling factors of a two-dimensional electron gas. In the structures studied here, critical behavior at integer filling factors has been established for different characteristics of luminescence. For sample $1D$ the oscillations are collected in three panels of Fig. 8. The energy shift of the lowest PL maximum shows an upward cusp at integer filling factors from 1 to 4, and downward convex curves between them. The most pronounced feature at $B=10.3$ T corresponds to $\nu=2$. At this magnetic field the linear shift of the PL maxima changes to the diamagnetic behavior typical for trions. From the magnetic field value corresponding to $\nu=2$ we derive the 2DEG density $n_e=5\times10^{11}$ cm^{-2} and calculate the expected fields for the set of integer filling factors. These fields are marked by vertical dotted lines in panels (a), (b), and (c). They are in good agreement with evaluations of ε_F and n_e derived from the linewidth of the emission line, which, however, are much less accurate. This also coincides well with data on the optical detection resonance spectroscopy with the use of far-infrared radiation performed for the same sample.[21]

Very pronounced features are observed for the even filling factors $\nu=2,4,6$ for the PL circular polarization degree, which exhibits a minimum when the number of Landau levels that are fully occupied for each spin are equal [Fig. 8(a)]. Also, the PL intensity in σ^+ polarization shows dips at $\nu=1$, 2 and 4 [Fig. 8(b)] and maxima at $\nu=2$ and 4 in σ^+ polarization. The integrated PL intensity also shows oscillatory behavior [Fig. 8(c)], which can be explained by a decrease of the radiative recombination rate at integer filling factors. However, this interpretation requires additional experimental support, e.g., time-resolved measurements of the emission decay. It is worth noting here that oscillatory behavior was also detected in experiments with nonresonant heating of a 2DEG by a far-infrared laser (184.3 μm).[21] Clear minima in the electron temperature were found for $\nu=2$ and 4, i.e., when electron acceleration within the same Landau level is prohibited because all the states are occupied. Figure 9 shows a summary of the oscillating properties for sample $2D$. In contrast to sample $1D$, oscillations of the lowest transition energy and of the total PL intensity are less pronounced. Landau-level broadening in the sample $2D$ is considerable, which indicates strong scattering of electrons by impurities and by electrostatic potential of ionized donors from modulation doped layers. Luminescence of the different Landau levels can be clearly separated only for magnetic fields above 15 T. Nevertheless, the 2DEG density can be derived by the analysis of the luminescence linewidth, which oscillates in phase with the Fermi energy for each electron spin in the corresponding circular polarization [see Figs. 9(a) and 9(b)]. The degree of circular polarization given in Fig. 9(a) also oscillates and shows pronounced minima at even filling factors and maxima at odd filling factors.

We now relate the experimental data from Fig. 6 to a simple fan chart diagram for transitions between Landau levels of conduction and valence bands. The energy positions of these transitions, labeled as $N_eN_h{}^{\sigma}$ are expected at

$$E^{\sigma}_{N_eN_h}=E_{\mathrm{FEE}}+\left(N_e+\tfrac{1}{2}\right)\hbar\omega_{ce}+\left(N_h+\tfrac{1}{2}\right)\hbar\omega_{ch}+E_z^{\sigma}. \quad (1)$$

Here E_{FEE} is the fundamental emission edge, which includes the band gap renormalization and the excitonic effect between electrons and photoholes. E_z^{σ} accounts for the Zeeman splitting of the valence and conduction band states. We use

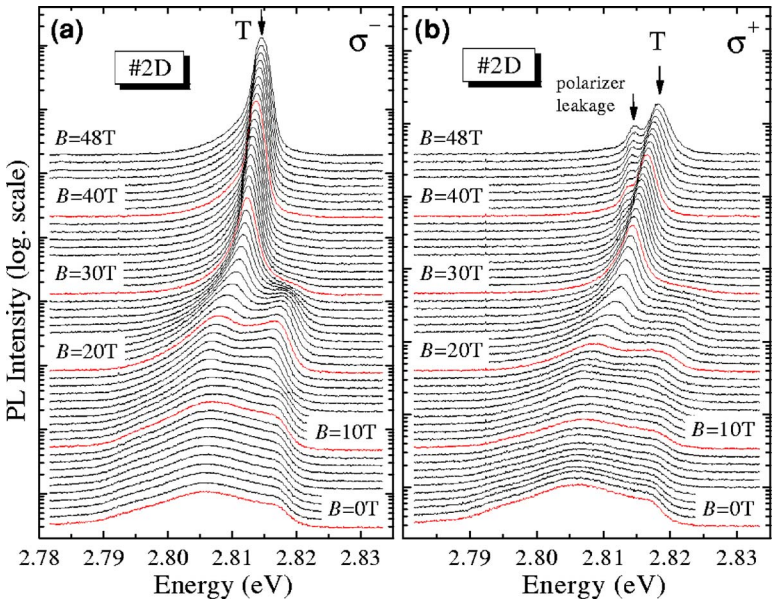

FIG. 7. (Color online) PL spectra from a doped 100-Å-thick $ZnSe/Zn_{0.94}Be_{0.06}Se$ QW $2D$ with $n_e=1.4\times10^{12}$ cm^{-2} for magnetic fields varied from 0 to 46 T and $T=1.6$K. (a) in σ^- polarization. (b) in σ^+ polarization.

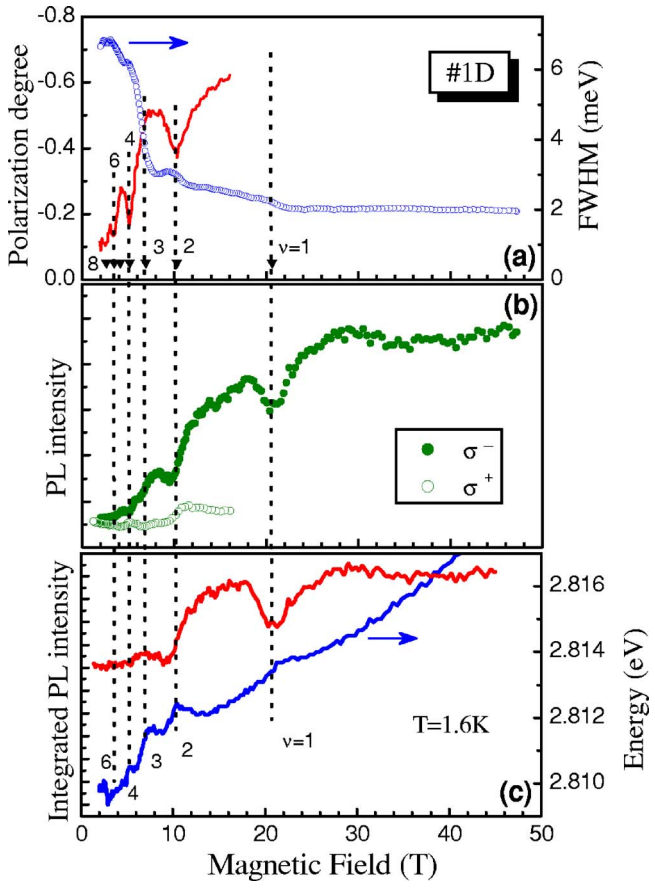

FIG. 8. (Color online) Summary of nonmonotonic behavior of the magneto-optical properties of a doped 67-Å-thick $ZnSe/Zn_{0.82}Be_{0.08}Mg_{0.10}Se$ QW $1D$ with $n_e=5\times10^{11}$ cm^{-2}: (a) polarization degree and linewidth of PL band; (b) PL intensity for two circular polarizations; (c) integrated emission intensity over both polarizations and energy shift of PL maxima detected in σ^- polarization. Dotted lines indicate locations of integer filling factors.

here the respective values determined for the reference samples and we do not account for the possible modification of the electron Zeeman splitting due to the electron-electron exchange interaction.[19] $\hbar\omega_{ce}=\hbar eB/m_e$ and $\hbar\omega_{ch}=\hbar eB/m_h$ are the cyclotron energies of the conduction band electrons and the valence band holes, respectively, and $N_{e(h)}=0,1,2,\ldots$, is the Landau-level number. While the selection rule $N_e=N_h$ pertains for light absorption (i.e., for PLE and reflectivity spectra), the rule can be violated for emission spectra by the carrier scattering with the Fermi sea electrons.

In Fig. 6 fan diagrams of emission lines in external magnetic fields are shown for two doped samples. The size of the symbols corresponds to the emission intensity. The symbol size at higher Landau levels ($N_e>0$) is 5 times magnified with respect to $N_e=0$. In low magnetic fields for $\nu>2$ the experimental data of both samples are described considerably well by Eq. (1) by supposing optical transitions between electrons from Landau levels $N_e=0,1,2,3,\ldots$, and holes from Landau levels $N_h=0$. The effective masses $m_e=0.15m_0$ and $m_h=0.46m_0$ were used for the calculation of emission energy given by solid lines, and E_{FEE} was treated as a fitting parameter. The best agreement with the experimental data for the sample $1D$ is achieved for $E_{\mathrm{FEE}}=2.808$ eV. This value coincides reasonably well with the low energy tail of the emission band at a zero field determined as $\mathrm{FL}-\varepsilon_F=2.8065$ eV (see also Fig. 1).

For the $1D$ sample the transformation to a diamagnetic behavior at $\nu<2$ takes place at $B=10.3$ T. It is instructive to compare in this regime emission spectra of the doped and reference samples. Modification of the magneto-optical spectra in ZnSe-based QWs with a low-density 2DEG has been studied in detail in Refs. 35 and 39. Dashed curves in Fig. 6(a) represent the shift of exciton and singlet trion states, measured for sample $1R$. The diamagnetic shift of these lines (i.e., quadratic with increasing magnetic fields) is characteristic for excitons and trion complexes. It is worth noting that the properties of the reference structure (energy shift, PL intensity, polarization degree) change smoothly with magnetic field, showing none of the cusps or jumps that are typi-

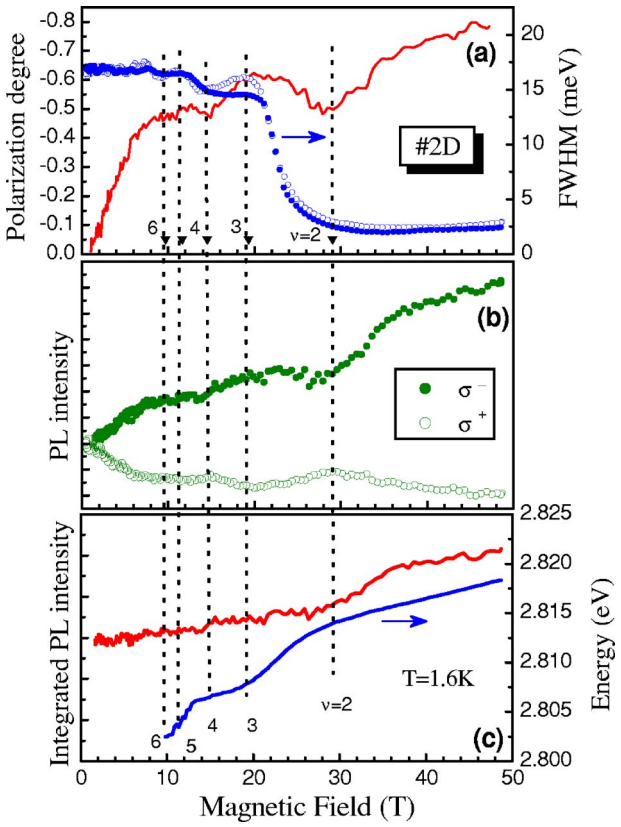

FIG. 9. (Color online) Summary of nonmonotonic behavior of the magneto-optical properties of a doped 100-Å-thick $ZnSe/Zn_{0.94}Be_{0.06}Se$ QW $2D$ with $n_e=1.4\times10^{12}$ cm^{-2}: (a) Polarization degree and linewidth of luminescence band; (b) PL intensity for two circular polarization; (c) integrated emission intensity over both polarizations, and energy shift of PL maxima detected in polarization. Dotted lines indicate locations of integer filling factors.

cal for doped samples. One can see that the strongest line of sample $1D$ shifts parallel to the trion line of the reference sample in wide field range from 10.3 up to 48 T corresponding to $\nu<2$. Also the second line, which appears for sample $1D$ at $\nu<1$ shows a quadratic diamagnetic shift that is parallel with the excitonic line of the reference sample. The energy offset between transitions in the doped and reference samples are 8 meV. As we will see below it is negligible for the second set of samples $2R$ and $2D$; therefore we believe that for the offset between samples $1R$ and $1D$ is mainly caused by the difference in QW widths caused by a growth inaccuracy.

Figure 6(b) shows the corresponding data for sample $2D$ with an electron density of $n_e=1.4\times10^{12}$ cm^{-2}. The situation is similar to the case of sample $1D$. In low magnetic fields for $\nu>2$ transitions energies show a reasonable agreement with the fan chart diagram. Due to the large broadening of the Landau levels the energy position of the transitions between the Landau levels cannot be resolved for higher filling factors $\nu>6$. Energies of the high energy cutoff of emission spectra (that involves electrons in vicinity of the Fermi level), are shown by squares. It is remarkable that again the fundamental emission edge $E_{\mathrm{FEE}}=2.797$ eV is equal to the low energy shoulder of the PL band $\mathrm{FL}-\varepsilon_F=2.7975$ eV (see also Figs. 2 and 3). Such a systematic behavior from both doped samples confirms our phenomenological description given in Fig. 12.

In magnetic fields above 28 T($\nu<2$) the energy of the main optical transition of $2D$ coincides with the trion energy in $2R$ [compare symbols with dashed lines in Fig. 6(b)]. The recovery of the exciton transition cannot be found in this plot as $\nu=1$ is expected at $B=58$ T which exceeds the highest field available for the used experimental facility.

B. Reflectivity spectra

We turn now to the discussion of the reflectivity spectra of the doped samples in external magnetic fields. The spectra from sample $1D$ in magnetic fields are given in Fig. 10. The shorter data acquisition times required by the pulsed field experiments do not allow resolution of the weak ω_2 resonances visible in Fig. 1(b). At $B=0$, the reflectivity spectra

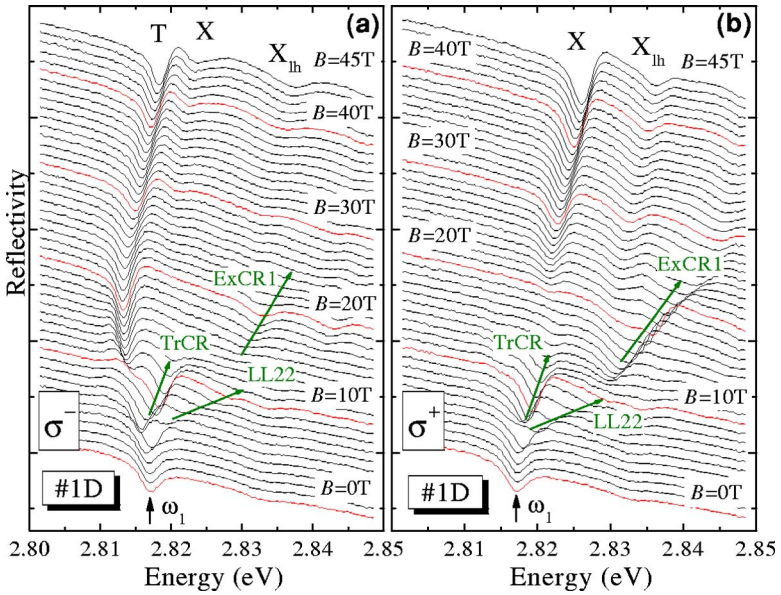

FIG. 10. (Color online) Reflectivity spectra of a doped 67-Å-thick $ZnSe/Zn_{0.82}Be_{0.08}Mg_{0.10}Se$ QW $1D$ with $n_e=5\times10^{11}$ cm^{-2} in a magnetic field range from 0 to 45 T at $T=1.6$ K. (a) σ^- polarization. (b) σ^+ polarization.

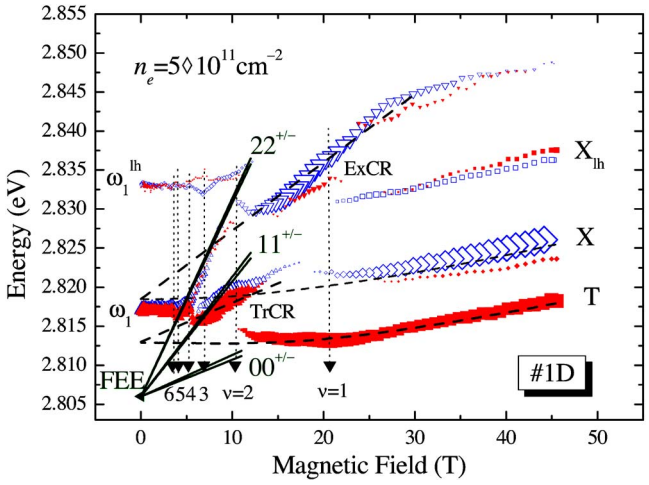

FIG. 11. (Color online) Energies of reflectivity lines vs magnetic field detected in σ^+ (open symbols) and σ^- (closed symbols) polarizations for a doped 67-Å-thick ZnSe/$Zn_{0.82}Be_{0.08}Mg_{0.10}Se$ QW 1*D* with $n_e=5\times10^{11}$ cm^{-2}. Intensities of resonances are displayed by the size of the symbols. Solid lines represent the Landau level fan chart for diagonal transitions with in-plane electron and hole effective masses of $m_e=0.15m_0$ and of $m_h=0.46m_0$, respectively. Vertical lines indicate locations of integer filling factors. The energy of the renormalized band gap at 2.8065 eV obtained from the extrapolation to zero field corresponds well to the energy position $\hbar\omega_1-(1+m_e/m_h)\varepsilon_F=2.8053$ eV. Dashed curves represent the quadratic diamagnetic shift of the trion and exciton as well as the energy of the combined TrCR and ExCR processes.

are dominated by the ω_1 resonances of the heavy-hole and light-hole transitions at 2.8169 and 2.8331 eV, respectively. In the high field limit, two heavy-hole transitions can be clearly seen, analogous to the exciton and trion resonances in the reference structure 1*R*. Additionally, the light-hole transition gains oscillator strength for both polarizations. In the following, we focus our discussion on the heavy-hole transitions. In σ^- polarization, the reflectivity spectra at high fields are dominated by the trion-like resonance. A weaker exciton-like resonance is recovered at filling factors $\nu<1$. In σ^+ polarization only the exciton-like resonance is restored for filling factors $\nu<1$. Polarization properties of the exciton-like and trion-like resonances coincide with the behavior of the reference sample. The strong circular polarization of the transitions originates from the complete spin polarization of the 2DEG for filling factor $\nu<1$. In this regime all electrons occupy states with spin $-\frac{1}{2}$. Trion singlet states have antiparallel electron configuration. As a result, this state can only be excited resonantly with σ^- polarized light (for details see Ref. 31).

At intermediate magnetic fields the ω_1 line transforms into a set of resonances, which shift approximately linearly with the magnetic field. The origin of these resonances is discussed in the following. Figure 11 shows resonance energies of reflectivity lines vs magnetic fields (symbols). The size of the symbols corresponds to the relative oscillator strength of the resonances. At low magnetic fields, the reflectivity spectra are dominated by the ω_1 resonance. At $\nu=5$, when the $N_e=2$ Landau level for electrons with spin +1/2 becomes depopulated, the ω_1 resonance starts shifting linearly to higher energies and loses its oscillator strength in σ^+ polarization. The slope of this shift is 2.5 meV/T. This value is in good agreement with the expected energy shift of diagonal transitions between electron and hole Landau-levels with $N_{e(h)}=2$, which should have a slope of 2.55 meV/T for $m_e=0.15m_0$ and of $m_h=0.46m_0$. Analogous to the PL data, it is instructive to compare the reflectivity data to a simple fan chart diagram derived from Eq. (1). The best agreement with the experimental data was achieved using $E_{\mathrm{FEE}}=2.8065$ eV. This value is very close to the expected energy position $\hbar\omega_1-(1+m_e/m_h)\varepsilon_F=2.8053$ eV.

The calculated transitions between Landau levels with $N_e=N_h$ are shown in Fig. 11 by solid lines. At $\nu=4$, where only two Landau levels for each spin are occupied, the main resonance shows a small redshift in σ^- polarization and σ^+ polarization, respectively. At $2<\nu<4$, the main resonances shift approximately linearly with slopes of 0.55 meV/T and 0.72 meV/T for the respective polarizations. These values deviate strongly from the expected slope of $N_e=N_h=1$ transitions, which is predicted to be about 1.5 meV/T. In samples with lower electron density at filling factor $2<\nu<4$ a combined process is observable in absorption and reflectivity in which an electron is excited from a filled Landau level to a higher empty Landau level during the creation of a trion. This four-particle process is known as a combined trion cyclotron resonance (TrCR) and has a slope of about $\frac{1}{2}\hbar\omega_{ce}$.[40,41] The energies of the TrCR line, extrapolated to a zero field, meets the energy of the "bare" trion, i.e., the energy obtained from the extrapolation of the quadratic diamagnetic shift of the trion to low magnetic fields (dashed line). This line should therefore have a trion origin.

At $\nu\leqslant2$ a new resonance gains oscillator strength in the reflectivity spectra, which is blueshifted with respect to the exciton resonance. From the slope it can be identified as a combined exciton-cyclotron resonance (ExCR).[42] This resonance is due to a process in which photocreation of a neutral exciton occurs simultaneously with a transition of a background electron between Landau levels. The ExCR line shifts linearly with magnetic fields as 0.9 meV/T (dashed line). Extrapolating to the zero-field limit, the ExCR line meets 2.8185 eV, which is the energy of the extrapolation of the quadratic diamagnetic shift of the exciton, as illustrated by a dashed line in Fig. 11. The ExCR slope of 0.9 meV/T is very close to 0.96 meV/T derived from the theoretical approach of Ref. 42, as $[1+m_e/(m_e+m_h)]\hbar\omega_{ce}$ with $m_h=0.46m_0$. As already mentioned, the size of the symbols in Fig. 11 reflects the relative oscillator strength of the resonances. One can see that the ExCR process gains its maximum oscillator strength close to the filling factor $\nu=1$, where the probability to find one (only one) electron in the orbit of photogenerated exciton is maximal. We should note here that in these experiments the exciton Bohr radius is still 1.5–2.5 times smaller than the magnetic length of electrons, which is 57 Å at 20 T.

Summarizing, reflectivity data show clear evidence of many-body interactions in low magnetic fields. The ω_1 resonance at the fundamental absorption edge transforms to a Landau-level behavior with $N_e=N_h$. In high magnetic fields,

however, exciton and trion resonances are restored in reflectivity spectra, and cyclotron shifts of the observed lines are well described in terms of combined ExCR and TrCR processes.

V. PHENOMENOLOGICAL PICTURE AND CONCLUSIONS

There are a number of numerical factors which must be taken into account in order to quantitatively model the magneto-optical spectra of QWs containing a 2DEG. Many of these factors result from many-body effects, and cannot, therefore, be treated analytically. Among them are band gap renormalization, screening of excitonic states, and perturbation of the 2DEG by the presence of a photohole. Performing such calculations is beyond the intended scope of this paper. We are not aware of any such calculations for II-VI QWs. However, one can formulate a phenomenological description of the observed optical spectra and their modification in magnetic fields for the regime $E_B^T \leqslant \varepsilon_F \leqslant E_B^X$. We present such a description here with an aim to qualitatively summarize the main trends observed in 2DEGs with strong Coulomb interactions.

Figure 12 summarizes a phenomenological picture of optical transitions and their evolution in magnetic field. The starting point in the scheme is the band gap of the undoped QW, i.e., the QW without a 2DEG and without any photocarriers. The presence of the 2DEG leads to band gap renormalization, i.e. to a decrease of the band gap which results from repulsive electron-electron interactions. In the presence of photoholes, excitons are formed, which are not fully screened in the considered regime of low and moderate electron densities. The lowest possible transition in emission will involve an electron from the very bottom of the 2DEG. It is denoted in the diagram as the fundamental emission edge (FEE). It is convenient to relate all other characteristic energies and spectral shifts to the E_{FEE}, as shown. The observed emission band arises from all electrons in the 2DEG, since the optical selection rules are partially relaxed and indirect transitions with $\Delta k \neq 0$ become possible. The upper edge of the emission band results from electrons at the Fermi level (this optical transition is labeled as "FL" in Fig. 12), and it is shifted by ε_F to higher energy from the FEE. For the case of optical absorption, direct transitions ($\Delta k = 0$) possessing stronger oscillator strength dominate. An absorbed photon moves an electron from the valence band into the empty states in the conduction band which are just above the Fermi energy of the 2DEG. Due to the finite hole mass, this absorption transition associated with the Fermi edge is blueshifted by $(1+m_e/m_h)\varepsilon_F$ from the FEE, or correspondingly, by $(m_e/m_h)\varepsilon_F$ from the emission transition labeled FL in Fig. 12. In the reflectivity and PLE spectra shown in this paper, this absorption transition leads to a fundamental absorption edge and is denoted by ω_1.

Magneto-optical spectra can also be qualitatively explained in the same terms (Fig. 12). The magnetic field splits the conduction and valence bands into Landau levels. Emission spectra arise from transitions between occupied Landau levels in the conduction band ($N_e = 0, 1, 2, \ldots,$) to the zeroth Landau level in the valence band ($N_h = 0$). They appear as

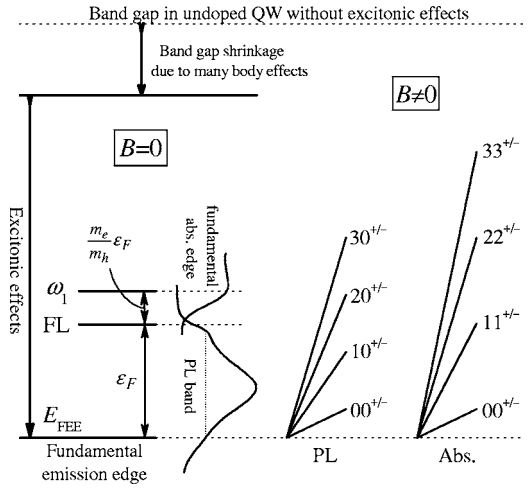

FIG. 12. Energetic hierarchy summarized from experimental data, which are obtained for QWs containing a 2DEG of moderate density.

local maxima in the emission band, which shift linearly with magnetic field. Extrapolating their shifts to zero magnetic field shows convergence on the FEE energy. In absorption spectra (i.e., reflectivity and PLE), only transitions with $N_e = N_h$ should become visible above ω_1, which implies transitions from the valence band to the unoccupied states in the conduction band. Extrapolating their energy shifts to zero field again exhibits convergence upon the FEE energy, similar to the emission lines. This phenomenological picture is valid for lower magnetic fields such that more than one Landau level is occupied by electrons, i.e., for filling factor $\nu > 2$.

In high magnetic fields, where $\nu < 2$, optical spectra are very similar to those from QWs with a very low electron density. One can see trionlike and excitonlike transitions shifting diamagnetically with increasing field. Also, combined processes of exciton-cyclotron and trion-cyclotron resonances become visible.

In conclusion, we have presented a detailed experimental study of the PL, PLE, and reflectivity spectra of ZnSe-based QWs containing 2DEGs at various temperatures and in high magnetic fields. We focused here on modulation-doped QWs with moderate 2DEG density, such that the Fermi energy falls in the range between the trion and exciton binding energies $E_B^T \leqslant \varepsilon_F \leqslant E_B^X$. To the best of our knowledge, a quantitative theory that describes the magneto-optical spectra of such 2DEGs does not yet exist. According to the experimental data presented in this paper, such a theory must account for excitonic effects that are modified by the many-body response of the 2DEG. We hope that our findings will encourage theoretical efforts toward a better understanding of this challenging field.

ACKNOWLEDGMENTS

The authors are thankful to H. A. Nickel and B. D. McCombe for collaboration at initial stages of this study and to V. P. Kochereshko for useful discussions. The work was supported by the Deutsche Forschungsgemeinschaft (SFB 410).

[1] I. V. Kukushkin and V. B. Timofeev, Adv. Phys. **45**, 147 (1996).
[2] S. Schmitt-Rink, D. S. Chemla, and D. A. B. Miller, Adv. Phys. **38**, 89 (1989).
[3] J. A. Brum, G. Bastard, and C. Guillemot, Phys. Rev. B **30**, 905 (1984).
[4] T. Uenoyama and L. J. Sham, Phys. Rev. B **39**, 11044 (1989).
[5] G. D. Mahan, Phys. Rev. **153**, 882 (1967).
[6] P. Hawrylak, Phys. Rev. B **44**, 3821 (1991).
[7] S. A. Brown, J. F. Young, J. A. Brum, P. Hawrylak, and Z. Wasilewski, Phys. Rev. B **54**, R11082 (1996).
[8] J. A. Brum, S. A. Brown, P. Hawrylak, J. F. Young, and Z. Wasilewski, Surf. Sci. **361**, 424 (1996).
[9] E. I. Rashba and M. D. Sturge, Phys. Rev. B **63**, 045305 (2000).
[10] R. A. Suris, V. P. Kochereshko, G. V. Astakhov, D. R. Yakovlev, W. Ossau, J. Nurnberger, W. Faschinger, G. Landwehr, T. Wojtowicz, G. Karczewski, and J. Kossut, Phys. Status Solidi B **227**, 343 (2001).
[11] M. S. Skolnick, J. M. Rorison, K. J. Nash, D. J. Mowbray, P. R. Tapster, S. J. Bass, and A. D. Pitt, Phys. Rev. Lett. **58**, 2130 (1987).
[12] G. Finkelstein, H. Shtrikman, and I. Bar-Joseph, Phys. Rev. B **56**, 10326 (1997).
[13] D. Gekhtman, E. Cohen, A. Ron, and L. N. Pfeiffer, Phys. Rev. B **54**, 10320 (1996).
[14] H. W. Yoon, M. D. Sturge, and L. N. Pfeiffer, Solid State Commun. **104**, 287 (1997).
[15] J. X. Shen, Y. Oka, W. Ossau, F. Fischer, A. Waag, and G. Landwehr, Physica B **249–251**, 589 (1998).
[16] V. Huard, R. T. Cox, K. Saminadayar, A. Arnoult, and S. Tatarenko, Phys. Rev. Lett. **84**, 187 (2000).
[17] V. Huard, R. T. Cox, K. Saminadayar, C. Bourgognon, A. Arnoult, J. Cibert, and S. Tartarenko, Physica E (Amsterdam) **6**, 161 (2000).
[18] G. V. Astakhov, V. P. Kochereshko, D. R. Yakovlev, W. Ossau, J. Nurnberger, W. Faschinger, and G. Landwehr, Phys. Rev. B **62**, 10345 (2000).
[19] A. Lemaitre, C. Testelin, C. Rigaux, T. Wojtowicz, and G. Karczewski, Phys. Rev. B **62**, 5059 (2000).
[20] Y. Imanaka, T. Takamasu, G. Kido, G. Karczewski, T. Wojtowicz, and J. Kossut, J. Cryst. Growth **214/215**, 240 (2000).
[21] W. Ossau, D. R. Yakovlev, G. V. Astakhov, A. Waag, C. J. Meinig, H. A. Nickel, B. D. McCombe, and S. A. Crooker, Physica E (Amsterdam) **12**, 512 (2002).
[22] R. T. Cox, R. B. Miller, K. Saminadayar, and T. Baron, Phys. Rev. B **69**, 235303 (2004).
[23] R. T. Cox, V. Huard, C. Bourgognon, K. Saminadayar, S. Tatarenko, and R. B. Miller, Acta Phys. Pol. A **106**, 287 (2004).
[24] D. R. Yakovlev, G. V. Astakhov, W. Ossau, S. A. Crooker, and A. Waag, in *Optical Properties of 2D Systems with Interacting Electrons*, NATO Advanced Studies Institute Series II, Physics and Chemistry, edited by W. J. Ossau and R. A. Suris, (Kluwer Academic Publishers Dordrecht, 2003), Vol. 119, p. 137.
[25] L. Calcagnile, R. Rinaldi, P. Prete, C. J. Stevens, R. Cingolani, L. Vanzetti, L. Sorba, and A. Franciosi, Phys. Rev. B **52**, 17248 (1995).
[26] G. Coli, L. Calcagnile, P. V. Giugno, R. Cingolani, R. Rinaldi, L. Vanzetti, L. Sorba, and A. Franciosi, Phys. Rev. B **55**, R7391 (1997).
[27] G. Kioseoglou, J. Haetty, H. C. Chang, H. Luo, A. Petrou, T. Schmiedel, P. Hawrylak, Phys. Rev. B **55**, 4628 (1997).
[28] M. A. Lampert, Phys. Rev. Lett. **1**, 450 (1958).
[29] K. Kheng, R. T. Cox, Y. Merle d'Aubigne, F. Bassani, K. Saminadayar, and S. Tatarenko, Phys. Rev. Lett. **71**, 1752 (1993).
[30] G. Finkelstein, H. Shtrikman, and I. Bar-Joseph, Phys. Rev. Lett. **74**, 976 (1995).
[31] G. V. Astakhov, D. R. Yakovlev, V. P. Kochereshko, W. Ossau, J. Nurnberger, W. Faschinger, and G. Landwehr, Phys. Rev. B **60**, R8485 (1999).
[32] R. A. Sergeev, R. A. Suris, G. V. Astakhov, W. Ossau, and D. R. Yakovlev, Eur. Phys. J. B **47**, 541 (2005).
[33] J. A. Brum and P. Hawrylak, Comments Condens. Matter Phys. **18**, 135 (1997).
[34] G. Yusa, H. Shtrikman, and I. Bar-Joseph, Phys. Rev. B **62**, 15390 (2000).
[35] G. V. Astakhov, D. R. Yakovlev, V. P. Kochereshko, W. Ossau, W. Faschinger, J. Puls, F. Henneberger, S. A. Crooker, Q. McCulloch, D. Wolverson, N. A. Gippius, and A. Waag, Phys. Rev. B **65**, 165335 (2002).
[36] V. Huard, S. Lovisa, R. T. Cox, K. Saminadayar, M. Potemski, A. Arnoult, J. Cibert, S. Tatarenko, and A. Wasiela, Physica B **256–258**, 136 (1998).
[37] G. V. Astakhov, V. P. Kochereshko, D. R. Yakovlev, W. Ossau, J. Nurnberger, W. Faschinger, G. Landwehr, T. Wojtowicz, G. Karczewski, and J. Kossut, Phys. Rev. B **65**, 115310 (2002).
[38] S. A. Crooker, D. G. Rickel, S. K. Lyo, N. Samarth, and D. D. Awschalom, Phys. Rev. B **60**, R2173 (1999).
[39] D. R. Yakovlev, G. V. Astakhov, W. Ossau, S. A. Crooker, K. Uchida, N. Miura, A. Waag, N. A. Gippius, A. Yu. Sivachenko, and A. B. Dzyubenko, Phys. Status Solidi B **227**, 353 (2001).
[40] W. Ossau, V. P. Kochereshko, G. V. Astakhov, D. R. Yakovlev, G. Landwehr, T. Wojtowicz, G. Karczewski, and J. Kossut, Physica B **298**, 315 (2001).
[41] V. P. Kochereshko, G. V. Astakhov, D. R. Yakovlev, W. Ossau, W. Faschinger, and G. Landwehr, Phys. Status Solidi B **229**, 543 (2002).
[42] D. R. Yakovlev, V. P. Kochereshko, R. A. Suris, H. Schenk, W. Ossau, A. Waag, G. Landwehr, P. C. M. Christianen, and J. C. Maan, Phys. Rev. Lett. **79**, 3974 (1997).